Turkish Journal of Electrical Engineering & Computer Sciences

http://journals.tubitak.gov.tr/elektrik/

Research Article

Turk J Elec Eng & Comp Sci
(2015) 23: 1142 – 1158

doi:10.3906/elk-1212-37

Energy management of solar car in circuit race

Erkan ATMACA*
Department of Electrical and Electronics Engineering, Faculty of Engineering, İstanbul University, Avcılar, İstanbul, Turkey

Received: 06.12.2012 • **Accepted/Published Online:** 24.07.2013 • **Printed:** 10.06.2015

Abstract: This study develops an optimal driving strategy for solar car on a track with nonzero gradients and sharp corners. This strategy consists of finding the racing line and the speed profile that minimizes the lap time with a given amount of energy. The problem is formulated in proper form for a commercial nonlinear optimization software program. The track is modeled into segments identified by their spatial coordinates on its own surface. The speed-distance behavior of the vehicle is linearized at each segment. The constraints set by the brushless DC motor, battery, and circuit are formulated accordingly. This is the motor type widely used in electric cars. The solver produces both the positions of the car on the track and entry speeds into the segments, which minimizes the lap time for the given amount of the solar power and battery reserve. The positions of the car describe the best racing line. Formulation of the constraints allows extracting the motor current profile from the speed profile, which comprises the set of control actions. These profiles help the human driver identify where and how much to accelerate along the track for the desired performance of the car. The algorithm presented here can also serve as a tool to assess the performance of an electric car at different road conditions, thus helping to choose the best settings of the motor and the car.

Key words: Minimum time maneuvering, circuit race, optimal speed profile, optimal racing line, energy management, nonlinear constrained optimization

1. Introduction

In the literature, several mathematical algorithms are reported for solar car management in long-distance races. Howlett et al. formulated the problem on a level road and described a power-hold-coast-brake strategy with lower and upper critical speeds [1]. Pudney showed that the best practical strategy is still a speed-holding strategy even on undulating roads and with an inefficient battery [2]. Pudney et al. improved this result with a realistic battery model, proposing that the optimal strategy is a critical speed strategy, which might change with solar power during the journey [3]. Wright proposed a constant speed strategy despite weather fluctuations [4]. Mocking and De Geus used numerical optimization techniques or heuristics, which search for a speed profile based on weather predictions during the race [5,6].

In long-distance races, the car is driven with small speed variations in response to road conditions and solar power. This strategy is interrupted by a few stops and speed limits during the journey. This leads to the fact that the car should be designed and driven for maximum efficiency, while cruising within a limited range of speed.

For a circuit race, the constant-speed strategy still holds if the track does not have sharp corners or steep

*Correspondence: erkana@istanbul.edu.tr

sections. Although unpredictability of the weather encourages the teams to design their cars for maximum efficiency with 2–5 kW motor power, sharp corners require the car to be capable of high acceleration, braking, and cornering performance. Frequent accelerating and braking actions lead to large and rapid rises and drops in motor current, and thus motor efficiency cannot be accepted as constant. Therefore, the optimal driving strategy in a circuit race is an acceleration-control strategy rather than a speed-hold strategy.

Due to its essential differences, formula racing provides insufficient guidance for optimal timing of a solar car in circuit racing. In formula races, expert drivers force the car up to its limits, where energy management is of secondary importance. Aerodynamic design allows high cornering speeds due to the downward forces on the car. With engine powers of up to 750 kW, the road gradients have practically no effects on the performance of the car. On the other hand, circuit racing conflicts with the motor choice of a highly efficient solar car. Adcock et al. verified through simulation and testing that increasing the motor power improves lap time at the expense of reducing the achievable range considerably [7].

One other source of guidance is the studies on optimal driving strategies of the trains on a track of nonzero gradient and with speed limits [8–10]. However, they search for solutions along prescribed paths, and in their current formulation, they are relevant to long-distance solar car events and are not directly applicable to circuit events.

There exist a couple of works handling solar car management in circuit racing. Ersöz predicted the performance of the car by developing a speed distribution model for the track [11]. Ustun et al. compared the energy consumptions and timings of the predefined driving scenarios [12]. However, they still did not propose a dedicated method for finding the speed and control profile of a solar car in circuit racing.

This study presents a method to calculate the optimal lap timing of a solar car in a circuit race. The speed profile with its racing line is generated for the best lap time at a given solar power input and energy constraint. The current profile is derived using the constraints and the speed profile. The track is modeled in segments, which are sized properly so that the speed-distance function of the car can be linearized. The lap time, the work done by the motor, the energy drawn from the battery, and the constraints are formulated in terms of this function. The independent variable is the distance. A nonlinear programming software program (NLP) can incorporate this formulation. This study uses the function fmincon in MATLAB.

Managing the battery charge content is the essence of the energy management of a solar car. The temperature and rate of discharge affect the apparent capacity of a lithium polymer battery. The Peukert relation is invalid for these batteries. In addition, the terminal voltage is an inadequate indicator of the battery energy content. Due to these complexities, this study makes a conservative assumption on the energy capacity of the package and takes it as a constant, which is estimated at a rate higher than the average rate of discharge.

For high efficiency, the solar car is built with zero lift design and low rolling-resistance tires. Since these tires have a reduced grip, the car tends to follow safe cornering speeds in order to handle the lateral forces. Therefore, the car can be modeled as a point mass, ignoring the yaw moments. In addition, the suspension elements can be assumed stationary with respect to the chassis, and the effect of suspension dampers on vehicle performance can be omitted. Only the accelerating and braking actions are taken into account.

2. Method

2.1. Minimum time maneuvering problem

Consider that the independent variable is the distance x. The states will then be $S(x) = (t(x), v(x), W(x))$, where $W(x)$ is the energy use out of the battery, and $t(x)$ and $v(x)$ are the time and speed of the car at x. The distance traversed around the track is X. Assume that there is a control $u(x)$ that minimizes $T = t(X)$.

In order to make use of the existing numerical solvers, this optimal control problem can be converted to a nonlinear programming problem by replacing the control and state histories with their discrete approximations.

Assume that there is an optimal racing line on the track. It can be divided into N segments as in Figure 1, which is sized suitably so that the optimal speed profile $v(x)$ at each interval $(x_i - x_{i+1})$ can be described by its linear approximation. The states and constraints can then also be formulated accordingly. The problem is to find the motor control action, which is the current I_i or power P_i at each interval $(x_i - x_{i+1})$ that minimizes the lap time T. The problem then turns into finding the speed profile:

$V_p = [v_0 \ v_1 \ v_2 \ \ldots \ v_N]$, such that lap time T is minimized where T_i is the time elapsed on interval (x_i - x_{i+1}):

$$T = T_1 + T_2 + \ldots . + T_N \tag{1a}$$

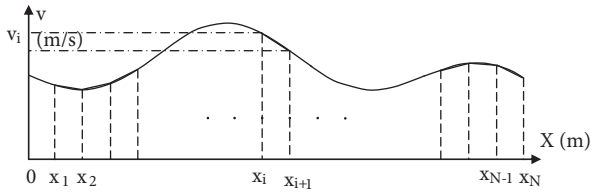

Figure 1. Optimal speed profile and its approximation.

The speed profile and its associated control profile must satisfy the following constraints:

- At each location x_i there is a speed constraint: amount of core losse

$$v_i <= V_i \tag{1b}$$

- $W_T = W_1 + W_2 + \ldots . + W_N$, where W_i is the energy use at segment $(x_i - x_{i+1})$

The energy available for each lap is constrained:

$$W_T <= W_{lap} \tag{1c}$$

$$v_0 = v_{N+1} \tag{1d}$$

The current and power of the motor is limited:

$$I_{M\,\min} <= I_i <= I_{M\,\max}, P_{M\,\min} <= P_i <= P_{M\,\max} \tag{1e}$$

2.2. Constraints imposed by the motor

Figure 2 shows the operating characteristics of the brushless direct current (BLDC) motor installed in the car [13].

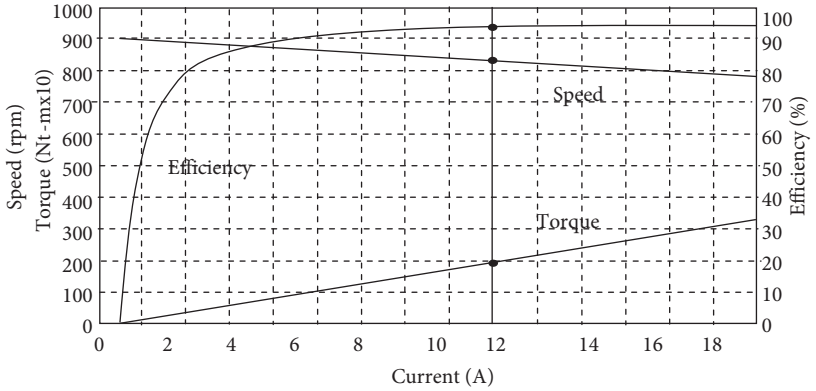

Figure 2. Speed, torque, and efficiency of the BLDC motor with its controller at 96 V.

In the BLDC motor, voltage drop on the switching elements during commutation may be significant. As a result, the torque and back emf constants are not always equal to each other, in contrast to a conventional DC motor [14]. Its total efficiency is determined primarily by the winding losses in the motor and the switching losses in the controller. In order to take the switching losses into account, all voltage drops can be attributed to coil resistance. This can be estimated from the steady-state characteristics in Figure 2, which is given at 96 V. This assumption still allows the motor constants to be nearly equal to each other in the actual speed range. Figure 2 is the graphical representation of the test data supplied by the manufacturer. The vertical line on this figure represents the operating point, at which the motor revolves at 810 rpm supplying 20 Nt-m torque with 94% efficiency. From a series of operating points an equivalent resistance R can be found representing all the losses. The total loss can be stated as:

$$\Delta P = V_{bat} I_M - P_o - \Delta P_{core} \approx 3 I_w^2 R, \tag{2}$$

where P_o is the output power with $P_o = \mathrm{T}\omega$, I_w is the coil current, and ΔP_{core} is the core losses together with mechanical losses. The change in the amount of core losses is inconsiderable from no load to full load. The manufacturer supplies its value.

Electrical transients in the controller are much faster than the mechanical transients in the car. Thus, it can be assumed that during the accelerating and braking phases, the torque and emf constants are the same as in the steady state. These simplifications allow modeling the motor as a torque source.

The torque of the BLDC motor is proportional to its current. The torque constant is defined in terms of rms value of the winding current. Noting that the current into the controller is I_M, the torque constant is k_T, and the wheel radius is r, the force of the motor can be written as:

$$F_M = 3 k_T I_M \sqrt{2/3}/r. \tag{3}$$

The force balance of the car is

$$F_M = F_R + F_a, \tag{4}$$

where F_R is the total resistance force of the car:

$$F_R = mgC_{rr}(1 + v/44.7) + 0.5\rho c_D A v^2 + mgsin(\alpha). \tag{5}$$

Moreover, F_a is the accelerating force on it.

The first term in Eq. (5) is the rolling resistance force, where C_{rr} is a tire-specific coefficient, m is the mass, and g is the gravitational constant [15]. The second term is the aerodynamic drag force, where ρ is the air density, c_D is the drag coefficient related to the geometry of the car, and A is the frontal area of the car. The third term is the road gradient force, where α is the road slope angle.

Taking the segment size to be sufficiently small, the current and thus the force of the motor, F_M, can be assumed constant throughout the segment $(x_i - x_{i+1})$. In Figure 3, the motor overcomes all resistances and adds or removes kinetic energy from the car at each segment. The work done by the motor can be calculated as:

$$W_i = \int_{x_i}^{x_{i+1}} F_M dx = \int_{x_i}^{x_{i+1}} F_R(x)dx + 1/2m(v_{i+1}^2 - v_i^2). \tag{6}$$

The speed terms in F_R are stated as a linear function of x, v_i, and v_{i+1} at any point along the segment $(x_i - x_{i+1})$. The integral in Eq. (6) results in a quadratic function of the form

$$W_i = c_1 v_i^2 + c_2 v_{i+1}^2 + c_3 v_i v_{i+1} + c_4 v_i + c_5 v_{i+1} + c_6. \tag{7}$$

The coefficients in Eq. (7) are written in terms of the constants in Eq. (5) and the term x_{di}, where x_{di} refers to the length of the segment defined by $(x_i - x_{i+1})$. The average force from the motor is then obtained as:

$$F_{Mi} = W_i / x_{di}. \tag{8}$$

At each point along $(x_i - x_{i+1})$, F_{Mi} must satisfy:

$$F_{M\,\min} \leq F_{Mi} \leq F_{M\,\max}. \tag{9}$$

The minimum force in Eq. (6) is a negative term, set by the maximum regenerative current out of the motor. This current is less than the maximum forcing current due to the battery safety issues. The controller can adjust the maximum current up to a value limited by its design. The maximum speed at which the controller is still able to force the maximum current at full battery voltage is called critical speed. Beyond this speed, the current and torque start to drop due to the rise of back emf voltage. These constraints can be described in terms of the approximate linear speed-distance relation shown in Figure 3.

In a star-connected BLDC motor as shown in Figure 4, the back emf constant k_e can be found as:

$$k_e = e_M/\omega_M = \sqrt{2/3}(V_W - I_M R)/\omega_M, \tag{10}$$

where V_W is the voltage per winding at speed ω_M and R is the winding resistance. The motor torque constant, k_T, can be written as:

$$k_T = T/3/(\sqrt{2/3} I_M). \tag{11}$$

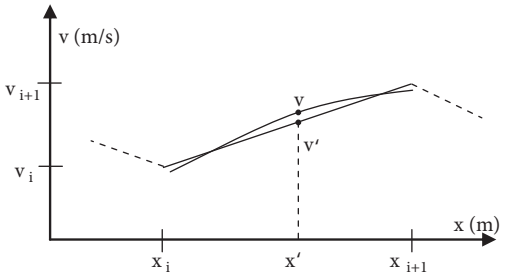

Figure 3. Linear approximation of the speed.

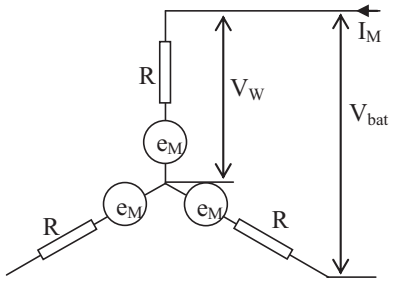

Figure 4. BLDC motor model.

By these definitions, the motor constants derived from the steady-state characteristics are approximately equal to each other over a wide range of speed:

$$k_M = k_T \sim k_e. \tag{12}$$

Combining Eqs. (10) and (11) and considering that the maximum value of V_W is $V_{bat}/2$, the maximum force at car speed v can be stated as:

$$F_{M\,\max} = (\sqrt{3/2}k_M/(rR))V_{bat} - 3k_M^2/(r^2R)v. \tag{13}$$

In Eq. (13) all terms except the speed term are constant. If the motor has field weakening capability, then the motor constant k_M will be a variable, too. At low speeds, the maximum force is constrained by the controller setting, while at high speeds it is constrained by the condition in Eq. (13).

2.3. Constraints imposed by the battery

In lithium-based batteries, energy capacity depends on the discharge rate, the temperature, and the age. Since the Peukert formula is not valid for these batteries, one practical solution for battery modeling is to assume a constant capacity estimated from the discharge rate predicted for a given loading condition. Since the controller limits the motor current, the maximum discharge rate can be assumed as less than 5C for each cell. According to the manufacturer's specification, the capacity of each cell is 14.7-W-h at 5C. If N_{cell} is the number of the cells, the total capacity of the package is then:

$$E_{batC} = 14.7N_{cell}W - h. \tag{14}$$

The energy reserve per lap depends on the organization of the race. In some races, teams should run a given number of laps in minimum time. In some others, teams run as many laps as possible in a specified period. The average solar power can be assumed constant if the time span of the race is short. The energy balance is then written as:

$$W_M = W_{lap} = E_{batC}/n + P_S T, \tag{15}$$

where W_M is the work done by the motor each lap plus winding losses, n is the number of laps, and P_S is the average solar power. If the time span of the race is long enough, then the energy balance can be written as:

$$W_M = W_{lap} = (E_{batC} + \int_{TR1}^{TR2} P_s(t)dt)/n. \tag{16}$$

In this case, n is the predicted number of laps and P_s (t) is a time-dependent function of the solar power. TR1 and TR2 are the beginning and ending times of the race. Eq. (16) is the interpretation of the speed-holding strategy in the long-distance race. Intuitively, it can be stated that in the circuit race, a constant profile of the speed holds each lap instead of a constant hold-speed along the entire track. At any instant during the race the energy storage in the battery must stay within the limits:

$$0 \leq E_{bat} \leq E_{batC}. \tag{17}$$

The current through the segment $(x_i - x_{i+1})$ can be found using Eqs. (3) and (8). Writing the total winding losses as

$$W_{Ri} = 3(\sqrt{2/3}I_M)^2 R, \tag{18}$$

the total energy consumption of the motor is:

$$W_{Mi} = W_i + W_{Ri}. \tag{19}$$

The amount of solar energy collected each interval depends on the time elapsed at that segment:

$$T_i = 2(v_i + v_{i+1})/x_{di}. \tag{20}$$

The energy use out of the battery can be written as

$$W_{Bi} = (W_{Mi} - P_S T_i)(1/\mu_B), \tag{21}$$

where W_{Mi} is the motor losses in addition to the work done on the car, and μ_B is the battery efficiency, which is less than one. Note that μ_B replaces $1/\mu_B$ if the energy is pumped into the battery. The battery constraint is written as:

$$W_B = W_{B1} + W_{B2} + \ldots + W_{BN} <= E_{batC}/n. \tag{22}$$

2.4. Selection of the segment size

Linearization of the speed causes an error $\Delta v = v - v\prime$ at any point, $x\prime$, over each segment as in Figure 5. To keep this error within acceptable bounds, the segments should be sized properly.

Setting the maximum error ε in speed over a segment as

$$\Delta v = v - v\prime; \varepsilon = \Delta v/v < 5e-5, \tag{23}$$

it is observed in numerous experiments that the segment size must be at most 1 m if the its entry speed, v_i, is 1 m/s. If the initial speed is 20 m/s then even a 98-m segment size is acceptable. These should be calculated specifically for each motor-car combination. The curved sections of the circuit should be modeled in detail with shorter segments, where high accelerations-decelerations are expected. In Appendix A (on the journal's website), it is shown that the linearization error in speed leads to an error in calculation of the power and energy consumption of the car as

$$\Delta P_R/P_R < 3\varepsilon. \tag{24}$$

2.5. Constraints imposed by the circuit

2.5.1. Modeling the circuit

Modeling of the circuit is a preliminary study. It is required to preserve the grade variations and curving properties of the circuit in its discrete model.

Google Earth facilitates the identification of the latitude and longitude of a point on the earth's surface. Using the functions of Google Earth, the centerline of the circuit can be represented in detail by sampling it at 1.5–5 m distances. The geodetic coordinates are then transformed into earth-centered Cartesian coordinates by a common ellipsoid model of the earth, GRS80 [16]. This study develops a second transformation based on three points forming a new Cartesian coordinate system on the track plane. Because of this transformation, the z-component of a point is the altitude of that point in the new frame. Note that the distance between two points does not change after these transformations.

2.5.2. Identifying the racing line

Figure 6 depicts a section of the best racing line on a hypothetical track, which the car follows with its consistent speed profile. The points C_i and C_i' identify the front line of the segment $(x_i - x_{i+1})$. These are the coordinates of the inner and outer lines of the circuit, which are at a distance half the width of the track on both sides from the centerline. These points represent a linear model of the circuit. They reflect the grade variations, curves, and corners of the circuit with reasonable accuracy.

The set of the points x_i forms the racing line that is searched for by the algorithm. The coordinates of the point x_i can be written in terms of K_i, which is the distance from the point C_i along the line $(C_i - C_i')$.

The circuit sets a speed limit at each point x_i such that

$$v_i^2 / r_{ci} \leq kg. \tag{25}$$

Here, r_{ci} is the radius of the curvature at point x_i, which is defined by the points x_{i-1}, x_i, and x_{i+1}. Here kg is the lateral acceleration limit for a safe cornering. Its value is found as nearly 0.55 g on analyzing the maximum actual speeds achieved during cornering on the circuits.

The locations x_i and x_{i+1}, the two points of varying positions on the two front lines, describe each segment. Thus, the length of a segment is a dependent variable given by

$$xd_i = |x_{i+1} - x_i| . \tag{26}$$

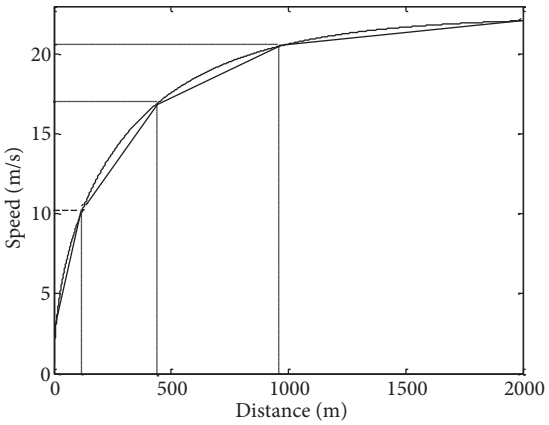

Figure 5. Acceleration profile.

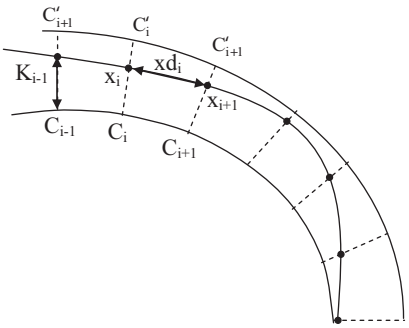

Figure 6. Racing line on a sample circuit.

2.6. Formulation of the solution

V_p is the vector representing all the variables searched for by NLP:

$$V_p = [v_1..v_{N+1}|\, K_1...K_{N+1}]\,, \tag{27}$$

where N is the number of segments. The circuit is coded by 2N+2 three-dimensional points. The first subvector represents the speeds; the second one represents the distances from the inner side of the circuit. The width of each segment sets the upper bounds for the terms in the second subvector.

The objective function and constraints described in Eq. (1) specify the problem of finding the minimum of a constrained nonlinear multivariable function. The variables are the entry speeds, v_i, and the distances from the inner line, K_i.

$$\min f(V_p), \tag{28a}$$

$$f(V_p) = \sum_{i=1}^{i=N} 2x_{di}/(v_i + v_{i+1}), \tag{28b}$$

where

$$x_{di} = |x_{i+1} - x_i|\,, \text{ and } x_i(x) = C_i(x) + K_{ix}; x_i(y) = C_i(y) + K_{iy}; x_i(z) = altitude(i). \tag{28c}$$

Here, (C_i(x), C_i(y), altitude(i)) are the coordinates of the inner point C_i in Figure 6; K_{ix} and K_{iy} are the x-axis and y-axis components of the distance K_i from the point C_i. The component altitude (i) is read from the model data of the circuit. The three-dimensional vector (x_i(x), x_i(y), x_i(z)) defines the coordinates of the point x_i, which is on a candidate racing line.

Using Eqs. (7) and (8) we can write the functions f_{di}:

$$f_{di} = c_{i1}v_i^2 + c_{i2}v_{i+1}^2 + c_{i3}v_iv_{i+1} + c_{i4}v_i + c_{i5}v_{i+1} + c_{i6}, i = 1, 2, \ldots, N.$$

The solution V_p^* must then satisfy the following nonlinear constraints, f_c, set by the motor:

$$f_c(i) : f_{di} \le f_{M\max}, \tag{29a}$$

$$f_c(i+N) : f_{di} \ge F_{M\min}, \tag{29b}$$

$$f_c(i+2N) : f_{di} \le F_{M\max}. \tag{29c}$$

The circuit sets a constraint at each point x_i:

$$f_c(i+3N) : v_i^2/r_{ci} \le kg. \tag{29d}$$

Finally, the solution must also satisfy the constraint set by the battery energy reserve and expected solar power, P_S:

$$f_c(4N+1) : \sum_{i=1}^{i=N} W_{Bi} = \sum_{i=1}^{i=N} (W_{Mi} - P_S T_i)/\mu_B \le \text{ batreserve}. \tag{29e}$$

In the above equations, the coefficients c_{ij}, j = 1...6, are determined by the car parameters and the term x_{di} in Eqs. (6–8). The maximum motor force at low speeds, $f_{M\max}$, is set by the controller:

$$f_{M\max} = 3I_{M\max}\sqrt{2/3}k_M/r. \tag{30}$$

The maximum motor force at high speeds, $F_{M\,\max}$, is determined by Eq. (13).

The solution V_p^* is bounded such that

$$0 \leq v_i \leq 30m/sec, and 0 \leq K_i \leq \text{ trackwidth, } i = 1, 2, \ldots, N. \tag{31}$$

Here, trackwidth is the width of the track, which is assumed as constant and equal throughout the circuit.

Three-dimensional coordinates of the points $(x_{i-1},\ x_i,\ x_{i+1})$ determine the radius of curvature at point x_i. To calculate it a MATLAB function is developed and integrated into the constraint functions.

In the constraint function f_c (4 N + 1), the work done by the motor along the segment $(x_i - x_{i+1})$, W_{Mi}, is calculated by Eqs. (6), (7), (18), and (19), while T_i is given by Eq. (20).

The solution must also satisfy the linear equalities:

$$v_1 = v_{N+1}, K_1 = K_{N+1}. \tag{32}$$

The objective function has an explicit form, and thus its derivative can be supplied to the solver. However, x_i is a variable and stated implicitly in terms of K_i. Therefore, it is complicated to formulate the derivatives of the constraint functions in Eq. (29). They have to be approximated by the solver itself using the finite differencing technique. As the number of segments increases, it may be computationally expensive. This is the main reason for modeling the circuit with the least number of points.

Operation of the algorithm is summarized in Figure 7.

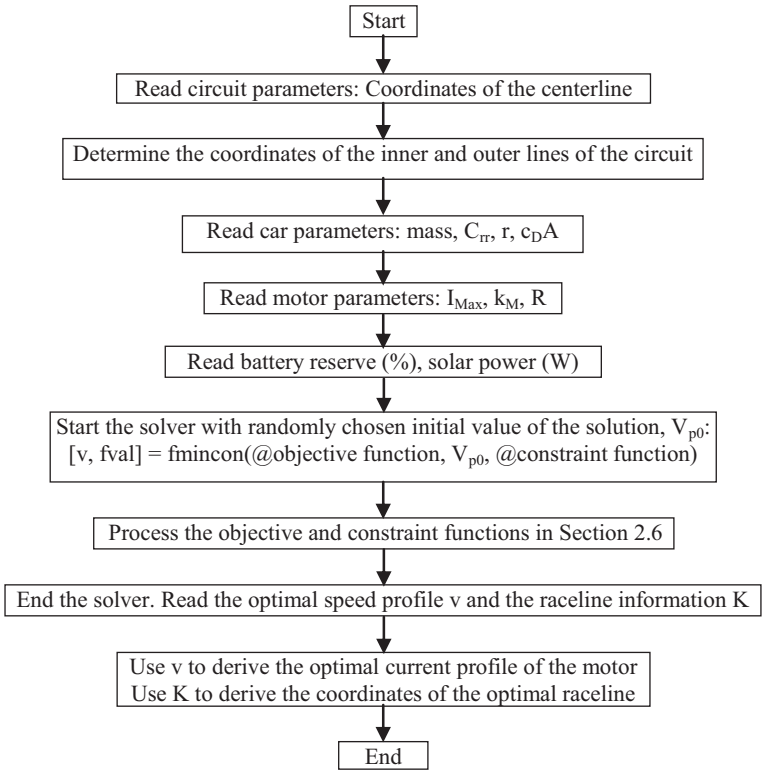

Figure 7. Operation of the algorithm.

3. Testing the method

3.1. Properties of the circuits and cars

The test circuit is almost a level track with sharp corners. Its properties in the linearized model are summarized in Table 1. The parameters of the test car are given in Table 2, where aerodynamic drag coefficient is found by computer analysis. Although the motor has regenerative braking capability, it is not used for battery safety. The nominal battery voltage is 122 volts in the tests.

Table 1. Properties of the test circuit.

Length (m)	Segment size (m)	# of segments	Altitude (m)	Slope (deg.)	Width (m)
1842	1.8–15.8	183	1.5–7.7	–3.8 to 3.7	12

Table 2. Properties and settings of the test car.

Total mass (kg)	c_D A	C_{rr}	r (m)	Motor constant	Max. current (A)
220	0.22	0.004	0.27	0.6	0–40

3.2. Testing the assumptions on a model track

The basic assumption in this study is that if the linearization of a circuit is sufficiently fine, then the optimal speed profile of a vehicle can be linearized also. This linearization then facilitates the formulation of the objective and constraint functions in a proper form for a common nonlinear optimization software program.

Two demonstrative cases are considered to test the validity of the models and assumptions used in the study. The battery is perfectly efficient, while the motor has a variable efficiency.

3.2.1. Test case 1: Travel on a track with steep gradients

Daniels et al. developed the most efficient speed profiles for a track with steep gradients formulating the motion of the car as an optimal control problem [17]. Those profiles can be taken as a benchmark case for testing purposes. Consider a track whose first 450-m section is level. It is followed by a 50-m uphill section with gradient of 6%. After that, a 490-m level section stretches again. In the second part of this test, the uphill section of the track is replaced by a downhill section with gradient –6%. The number the segments representing the track is 110, each of which is 9 m.

Figure 8 shows the speed profiles of the test car on this steep track. These have the same characteristics as presented by Daniels et al. [17]. For optimal use in hilly road conditions, the car in a constant hold-speed starts to accelerate gradually to the beginning of the uphill section, through which it loses some of its kinetic energy. At the end of that section, it accelerates again up to the hold-speed. In the second part of the test, the car lowers it speed until the beginning of the downhill section, through which it gains some kinetic energy. At the end of the section, it decelerates again to the hold-speed. Note that the speed of the car is the same at the beginning and end of the track.

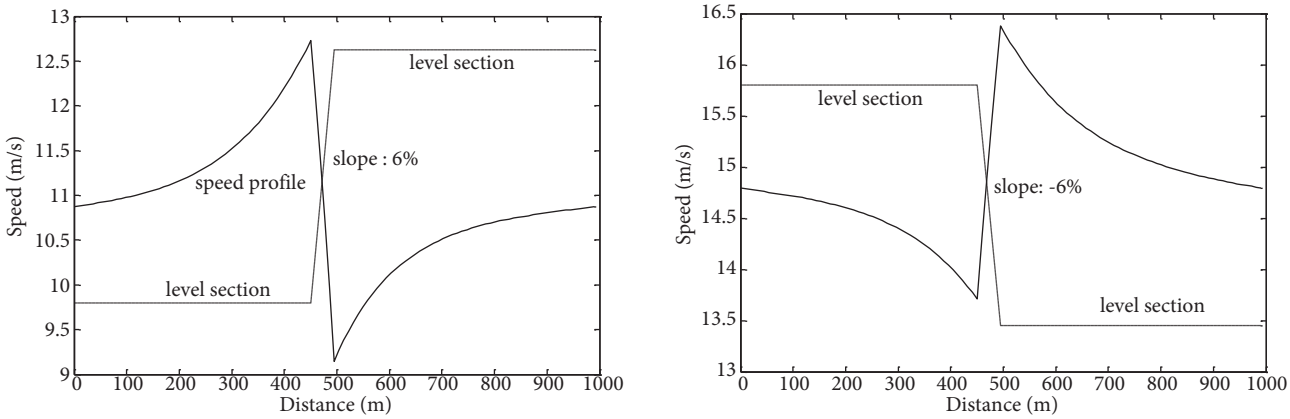

Figure 8. Speed profile on a hilly track: a) uphill section b) downhill section.

3.2.2. Test case 2: Travel on a level circular track

An entirely circular track significantly affects the cruising speed of a car. Since there is no case reported in literature, in Appendix B (on the journal's website), it is shown that on such a track as in Figure 9, a car always follows the inner circle in optimal use even if it has both high energy reserve and strong cornering capability. To test this expectation, assume a circular track with a 326.2-m centerline that is represented in 40 segments.

If the lateral acceleration constraint, kg, is set to 0.72 g, then the test car can travel at speed 18 m/s around the inner circle with a 7.5 W-h energy consumption. Here, g is the gravitational constant. The radius of the inner circle is 45.9 m. When the algorithm is run with these constraints, it results in a constant-speed profile of 18 m/s with up to 4e-3 m/s errors while the car traverses the inner circle. Now we double the energy reserve and reduce the cornering capability to 0.64 g, which provokes the car to turn at a larger radius with a higher speed. Subject to these new constraints, the algorithm results in a constant-speed profile of 16.97 m/s around the inner circle with energy consumption of 6.94 W-h, which is less than the previous one. In this case, the turning radius is 45.9 m again, which can be verified by setting v = 16.97 m/s at v^2 / (0.64 g). This is the expected result. Even if the energy reserve is high, the cornering constraint dominates at the optimal speed profile and adjusts it so that the car follows the inner circle. Thus, the algorithm is valid for a circular track as well.

3.3. Testing the method on a real track

3.3.1. Monitoring energy content of the battery

For a race with a specified number of laps, Eqs. (15) and (16) reveal that the total energy consumption at each lap should be equal. If the time span of the race is short enough, then the solar power can be assumed constant during the race. In this case, the amount of energy drawn from the battery at each lap should be equal. To ensure that this condition holds, the battery energy content should be monitored during the race. If n is the number of laps, the battery energy reserve is 1/n per lap regardless of the amount of the average solar power expected during the race time. For a battery capacity E_{batC}, which is estimated from the discharge rates predicted for the race, the nominal battery reserve is E_{batC} / n per lap.

To fulfill this, the battery current and voltage are measured and sent to a computer via a telemetry system with 250–350 ms periods. The maximum error in current measurement is 0.1 A at 50 A due to the saturation effects in the current sensors. A microcontroller processes the analog output of the sensor to calculate

the actual value of the current. The same microcontroller also makes the voltage measurement with errors up to 10 mV.

In Figure 10, the battery current and the voltage are assumed to change linearly with respect to time between the two successive measurements.

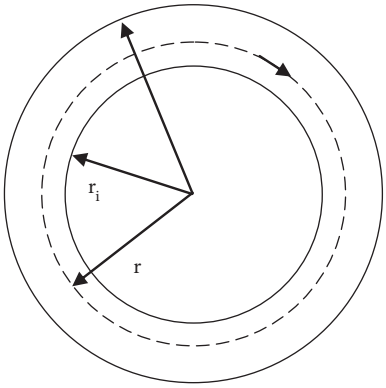

Figure 9. Travel on a circular track.

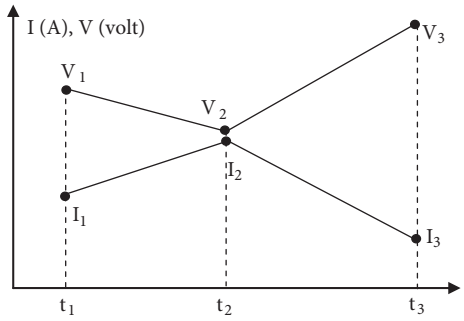

Figure 10. Current and voltage measurement.

The actual values are then approximated as:

$$i(t) = at + b; v(t) = ct + d; p(t) = v(t)i(t); W_{B1} = \sum_{t_1}^{t_2} p(t)dt, \tag{33}$$

In Eq. (33), (a, b) are stated in terms of (I_1, I_2, t_1, t_2), and W_{B1} is the amount of energy drawn from the battery in the first period. The accumulation starts at the beginning of the race and is checked at the end of each lap to make sure the energy consumption remains in a safe band around the battery reserve.

3.3.2. Estimation of solar power

Assume that for a given location the maximum power that a car can take is P_{Max} during the daytime. Between 0600 and 1800 hours the solar power can then be formulated as:

$$P_s(t) = P_{\max} sin(\pi/13t). \tag{34}$$

Here, t is set to 0 at 0600 hours and 13 at 1800 hours. The total solar energy between times t_1 and t_2 is $W_S = \int_{t_1}^{t_2} P_s(t)dt$. If time t_1 is the beginning time and t_2 is the approximate ending time of the race, then W_S / $(t_2 - t_1)$ is the average expected power during the race. The algorithm can be run with either the average-solar-power constraint or total-energy constraint. In the latter approach, the battery capacity is assumed to expand so that it stores all the energy reserve. While the solar power constraint is set to zero it is run with the same battery reserve per lap as in the previous case.

3.3.3. Test in a real circuit

Assuming a 30-lap race, the battery reserve per lap is 3.3%, or 31 W-h. Table 3 gives the performance of the car against solar power. At 1200 W, 0.5% of the reserve remains unconsumed. In this case, the total energy

consumption is 60.8 W-h. The average speed of the car per lap does not improve further despite the additional energy available. At the time of the test the official best time is 91.2 s, which is 1.8 s longer than the best performance predicted by the algorithm. In this lap, the racing line is 1795 m long, as given in Figure 11.

Table 3. Performance of the car as solar power increases.

Solar power (W)	Lap time (s)	Length of the racing line (m)	Battery use (%)	Solar energy use (W-h)	Total energy use (W-h)
0	120.0	1774	3.3	0.0	31.0
200	108.7	1778	3.3	6.0	37.0
400	101.4	1782	3.3	11.3	42.3
600	96.3	1786	3.3	16.1	47.1
800	92.3	1790	3.3	20.5	51.5
1000	89.5	1794	3.3	24.9	55.9
1200	89.4	1795	2.8	29.8	60.8

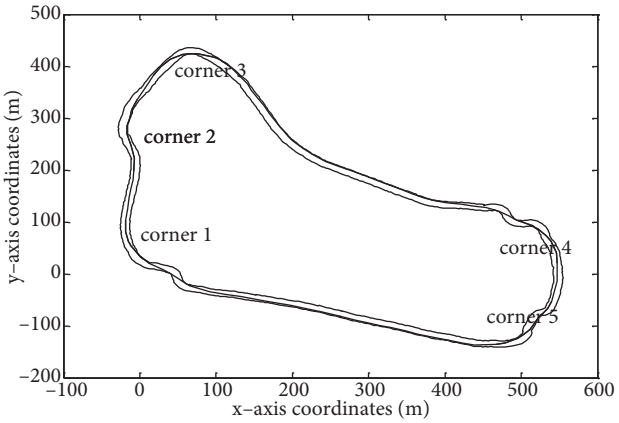

Figure 11. Racing line of the car: solar power is 1200 W.

The speed and current profiles for this lap are given in Figure 12. They demonstrate the positions of the acceleration and deceleration phases. At zero solar power, the racing line in Figure 13 tends to be the shortest path on the track. Figures 14a and 14b show the speed and the current profiles of the car. It is notable that almost the same pattern in each profile repeats itself as solar power increases. The lateral acceleration limit kg in Eq. (25) is identified by experience. It is set by checking the maximum safe speed into corner 3 in Figure 11. The maximum speed into this corner is measured between 55 and 60 km/h. The algorithm results in the speed of 58 km/h when kg is set to 0.50. The other cornering speeds predicted by the algorithm are also consistent with the measurements in the race.

4. Remarks

Note that the BLDC motor is operated in current-control mode. According to the manufacturer's specification, the current of the controller can be controlled linearly as long as the speed is under its critical value set by the condition in Eq. (12).

Although it is not an easy task to reproduce the speed and the current profiles in actual race conditions, these profiles help the human driver identify where and how much to accelerate along the track for the best performance of the car.

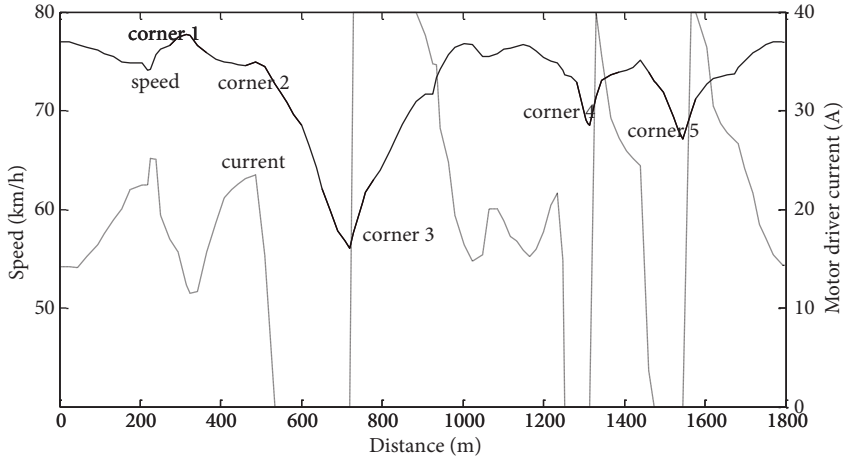

Figure 12. Speed and current profiles of the car: solar power is 1200 W.

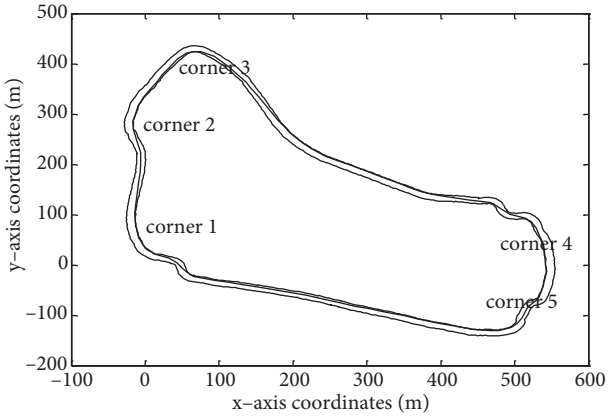

Figure 13. Racing line of the car: no solar power.

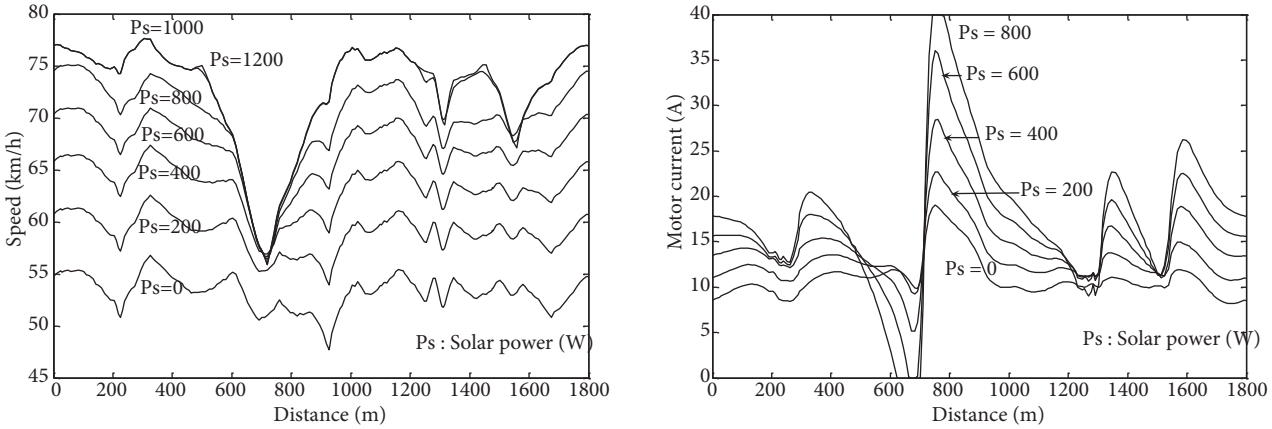

Figure 14. a) Speed profiles of the car as solar power increases. b) Current profiles of the car as solar power increases.

The number of segments modeling the circuit primarily affects the total computation time. With the numbers of segments given in Table 1, the algorithm searches for up to 368 variables. In this case, with a Pentium 3.4 GHz processor the computation times might change between 2 and 4 h for different energy constraints.

However, if it is assumed that the car follows a specified path, then the algorithm searches for only speed variables and as a result the total number of variables decreases to half. In this case, because the constraint functions are simplified, the algorithm can be speeded up further by providing the NLP with the derivatives of these functions. This process saves a considerable amount of time by avoiding the finite differencing calculations. For instance, the computation time may decrease down to 20–30 s.

There are two novelties in this study. First, to the best of the author's knowledge, this study is the first in the literature to investigate the energy management problem of solar car in circuit racing. The algorithm combines the search for the optimal speed profile with the search for its consistent path, a problem that is not a concern in long-distance races. Second, it models the motor as a torque source with variable efficiency unlike in long-distance events, where a constant efficiency model is sufficient.

The actual best lap times approximate the predictions within reasonable bounds. This validates the models used to describe the circuit, the motion of the car, and the motor.

The BLDC motor has a low weight-power ratio, which makes it proper for electric car applications. Therefore, the algorithm presented here can serve as a tool not only for solar car energy management but also for the performance evaluation of an electric car at different road conditions. With such a capability, it can help in choosing the best settings for both the car and the motor, like wheel radius, motor maximum current, and battery capacity.

The algorithm has room for improvement. It assumes a BLDC motor, and it needs modification to model the asynchronous motor as well, a second type of motor that is common in electric cars.

5. Conclusion

This work proposes an energy management strategy for a solar car in a circuit race. In a circuit race, the best performance depends not only on the optimal speed profile but also on its consistent path. This complicates the problem. Numerous near-optimal solutions can be found by actually driving the car on a given circuit, which is the case most of the time. However, this is an expensive and time-consuming experiment, and it might not always yield the true optimal result. On the other hand, this study assures a reliable solution to the energy management of a solar car and predicts its best possible performance. Finding the optimal speed profile with its consistent racing line, the algorithm guides the driver towards using the energy in the most efficient way. Other than its racing aspect, the algorithm given in this work can also serve as a tool for the performance evaluation of the electric car at different road conditions. Simulating the actual paths that are frequently used in an urban area as a circuit, this tool is proper for the performance testing of various settings of the car, the motor, and the battery.

Acknowledgments

The author would like to acknowledge the İstanbul University Scientific Research Unit for financial support of this research under grants 1341 (2009), 6986, 7083 (2010), 16308, 16359, 16402 (2011), and 25302 (2012), as well as the Ashiya University Solar Car Project Team in Japan for their contributions to this study.

References

[1] P. Howlett, P. Pudney, "Optimal driving strategy for a solar car on a level road", IMA Journal of Mathematics Applied in Business and Industry, Vol. 8, pp. 59–81, 1997.

[2] P. Pudney, Optimal energy management for solar-powered cars, PhD, University of South Australia, Adelaide, Australia, 2000.

[3] P. Pudney, P. Howlett, "Critical speed control of a solar car", Optimization and Engineering, Vol. 3, pp. 97–107, 2002.

[4] G.S. Wright, "Optimal energy management for solar car race", IEEE 39th Midwest Symposium on Circuits and Systems, Vol. 3, pp. 1011–1014, 1996.

[5] C. Mocking, Optimal design and strategy for the SolUTra, MSc, University of Twente, Enschede, the Netherlands, 2006.

[6] V. De Geus, "World Solar Challenge: The race strategy explained", SIGEVOlution, Vol. 2, pp. 8–11, 2007.

[7] P. Adcock, C.M. Crewe, N. Grange, M.A. Passmore, "Performance predictions for a single seater junior formula electric racing car", IEE Colloquium on System for Electric Racing Vehicles, pp. 8/1–8/7, 1993.

[8] P. Howlett, "Optimal control of a train", Annals of Operations Research, Vol. 98, pp. 65–87, 2000.

[9] E. Khmelnitsky, "On an optimal control problem of train", IEEE Transactions on Automatic Control, Vol. 45, pp. 1257–1266, 2000.

[10] J.X. Cheng, J.S. Cheng, J. Song, P. Zhao, "Algorithm on optimal driving strategies for train control problem", 3rd World Congress on Intelligent Control and Automation, Vol. 5, pp. 3523–3527, 2000.

[11] E. Ersöz, Development of a racing strategy for a solar car, MSc, Middle East Technical University, Ankara, Turkey, 2006.

[12] O. Ustun, M. Yilmaz, C. Gokce, U. Karakaya, R.N. Tuncay, "Energy management method for solar car design and application", IEEE International Conference on Electric Machines and Drives, pp. 804–811, 2009.

[13] Mitsuba Corporation, Special Motor for Solar Car Instruction Manual Book, Motor Model: M2096D II, 2010.

[14] D. Lin, P. Zhou, Z.C. Cendes, "In-depth study of the torque constant for permanent-magnet Machines", IEEE Transactions on Magnetics, Vol. 45, pp. 5383–5387, 2009.

[15] D.R. Carroll, The Winning Solar Car, Warrendale, PA, USA, SAE International, 2003.

[16] https://geodesyattamucc.pbworks.com/f/grs80parameters.pdf.

[17] M.W. Daniels, P.R. Kumar, "The optimal use of the solar powered automobile", IEEE Control Systems, Vol. 19, pp. 12–22, 1999.

A. Appendix

The error in power calculation due to the error in speed.

Omitting the error in time due to the linearization of the speed, the error in the work done by the motor to overcome the resistance of the car is:

$$\Delta W/W \approx \Delta P_R/P_R, P_R = P_{RR} + P_{RA}, \tag{A.1}$$

where P_R is the total resistance power, P_{RR} is the rolling resistance power, and P_{RA} is the aerodynamic resistance power:

$$P_{RR} = mgC_{rr}v + mgC_{rr}/44.7v^2 = M_dv + M_d/44.7v^2, \tag{A.2}$$

$$P_{RA} = 0.5\rho c_D A v^3 = A_d v^3. \tag{A.3}$$

The error in rolling resistance power is ΔP_{RR} due to the error Δv in speed v.

$$P_{RR} + \Delta P_{RR} = M_dv + M_d/44.7v^2 + M_d\Delta v + M_d/44.7(\Delta v)^2 + 2M_d/44.7v\Delta v \tag{A.4}$$

Neglecting the higher order terms,

$$\Delta P_{RR} \approx M_d(\frac{2v}{44.7} + 1)\Delta v = M_d\beta\Delta v. \tag{A.5}$$

The speed range in the actual race conditions is $0 \leq v \leq 22$ m/s. This leads to:

$$\Delta P_{RR} < 2M_d\Delta v, \tag{A.6}$$

$$\frac{\Delta P_{RR}}{P_{RR}} < \frac{2M_d\Delta v}{M_dv + M_d/44.7v^2} < \frac{2M_d\Delta v}{M_dv} < 2\frac{\Delta v}{v} = 2\varepsilon. \tag{A.7}$$

The error in aerodynamic power is ΔP_{RA}:

$$P_{RA} + \Delta P_{RA} = A_d(v^3 + 3v^2\Delta v + 3v(\Delta v)^2 + (\Delta v)^3). \tag{A.8}$$

Neglecting the higher order terms,

$$\Delta P_{RA} \approx 3A_dv^2\Delta v, \tag{A.9}$$

$$\frac{\Delta P_{RA}}{P_{RA}} \approx \frac{3A_dv^2\Delta v}{A_dv^3} = 3\frac{\Delta v}{v} = 3\varepsilon. \tag{A.10}$$

Write the rolling resistance power as a ratio of the aerodynamic power:
$P_{RR} = \alpha P_{RA}$.

$$\frac{\Delta P_R}{P_R} = \frac{\Delta P_{RR} + \Delta P_{RA}}{P_{RR} + P_{RA}} < \frac{2\varepsilon P_{RR} + 3\varepsilon P_{RA}}{P_{RR} + P_{RA}} = \frac{2\varepsilon\alpha P_{RA} + 3\varepsilon P_{RA}}{\alpha P_{RA} + P_{RA}} = \frac{2\alpha + 3}{\alpha + 1}\varepsilon \tag{A.11}$$

The factor α changes in actual speed range as the following:

$$0 < v < 30; 50 > \alpha > 0.1. \tag{A.12}$$

Thus, it results in:

$$\Delta P_R/P_R < 3\varepsilon. \tag{A.13}$$

B. Appendix

The optimal path of a car traveling on a circular track.

The problem of minimizing the lap time of a car on a circular track with no energy constraint can be stated as:

$$min(\frac{2\pi r}{\upsilon}), \tag{B.1}$$

subject to

$$\frac{\upsilon^2}{r} - kg \leq 0, r_i - r \leq 0, r - r_o \leq 0, \tag{B.2}$$

where υ is the optimal speed of the car, r is the radius of the path at the optimal speed, and r_i and r_o are the inner and outer radii of the track, respectively. The Lagrangian of this problem can be written as:

$$L = \frac{-2\pi r}{\upsilon} + \lambda_1(kg - \frac{\upsilon^2}{r}) + \lambda_2(-r_i + r) + \lambda_3(r_o - r). \tag{B.3}$$

The Kuhn–Tucker conditions for a point to be a minimum are:

$$\frac{\partial L}{\partial r} \leq 0, r \geq 0, r\frac{\partial L}{\partial r} = 0, \tag{B.4}$$

$$\frac{\partial L}{\partial \upsilon} \leq 0, \upsilon \geq 0, \upsilon\frac{\partial L}{\partial \upsilon} = 0, \tag{B.5}$$

$$\frac{\upsilon^2}{r} \leq kg, \lambda_1 \geq 0, \lambda_1(kg - \frac{\upsilon^2}{r}) = 0, \tag{B.6}$$

$$-r \leq -r_i, \lambda_2 \geq 0, \lambda_2(-r_i + r) = 0, \tag{B.7}$$

$$r \leq r_o, \lambda_3 \geq 0, \lambda_3(r_o - r) = 0. \tag{B.8}$$

The right-hand side terms in (B4) and (B5) are the complementary slackness conditions. In the explicit form these equations are written as:

$$\frac{-2\pi}{\upsilon} + \lambda_1\frac{\upsilon^2}{r^2} + \lambda_2 - \lambda_3 \leq 0, r \geq 0, \tag{B.9a}$$

$$r(\frac{-2\pi}{\upsilon} + \lambda_1\frac{\upsilon^2}{r^2} + \lambda_2 - \lambda_3) = 0, \tag{B.9b}$$

$$\frac{2\pi r}{\upsilon^2} - 2\lambda_1\frac{\upsilon}{r} \leq 0, \upsilon \geq 0, \tag{B.10a}$$

$$\upsilon(\frac{2\pi r}{\upsilon^2} - 2\lambda_1\frac{\upsilon}{r}) = 0. \tag{B.10b}$$

Since $\upsilon > 0$ and $r > 0$, Eq. (B.10a) requires $\lambda_1 > 0$. As a result, from Eq. (B.6),

$$\frac{\upsilon^2}{r} = kg.$$

If the car follows a path at optimal speed such that $r_i < \mathrm{r} < r_o$, then from Eqs. (B.7) and (B.8) it is written that $\lambda_2 = \lambda_3 = 0$. If this condition is put into Eq. (B.9b), it follows that $\lambda_1 = \frac{2\pi r}{kgv}$.

However, Eq. (B.10b) requires that $\lambda_1 = \frac{\pi r}{kgv}$. This is a contradiction. Thus, the condition $r_i < r < r_o$ does not hold. That is to say, the car will traverse the track either along the inner circle or the outer circle. Assume $r = r_o$. Thus, in Eq. (B.7) $\lambda_2 = 0$ and in Eq. (B.8) it follows that $\lambda_3 > 0$. From Eq. (B.10b) it results that $\lambda_1 = \frac{\pi r_o}{kgv}$. If this is put into Eq. (B.9b), then $\frac{-2\pi}{v} + \frac{\pi r_o}{kgv}\frac{kg}{r_o} - \lambda_3 = 0 \Rightarrow \lambda_3 = \frac{-\pi}{v}$. This is a contradiction because $\lambda_3 > 0$.

Now assume $r = r_i$. Thus, in Eq. (B.7) $\lambda_2 > 0$ and in Eq. (B.8) $\lambda_3 = 0$. Finally, Eq. (B.9b) results in $\lambda_2 = \frac{\pi}{v} > 0$. This result implies that the car will always traverse the circular track through the inner circle.